Journal of Mountain Area Research

Vol. 9, 2024

https://doi.org/10.53874/jmar.v9i0.177

Full length article

THE COMPARATIVE DEPOSITIONAL HETEROGENEITY OF MANCHHAR FORMATION (SIWALIK GROUP), SOUTHERN INDUS BASIN, PAKISTAN

Asghar A. A. D. Hakro[1], Aijaz Ali Halepoto[1], Muhammad Soomar Samtio[1], Riaz Hussain Rajper[1], Abdul Shakoor Mastoi[1], Rafique Ahmed Lashari[1], Mushtaque Ahmed Rahoo[1]*

1. Centre for Pure and Applied Geology, University of Sindh, Jamshoro

ABSTRACT

Present study is carried out for detailed description, distribution and interpretation of lithofacies and textural analysis of Manchhar Formation from Gaj River, Manchhar Lake and Lal Bagh Sections of Southern Indus Basin Pakistan. Four different clastic lithofacies are identified during present study, which are conglomeratic sandstone (Gt), shale (Fm), fine to coarse grain flat bedded sandstone (Sh) and fine to coarse grain trough cross-bedded sandstone (St). These Facies suggest that Manchhar Formation is deposited in the Beach to shallow agitated water and fluvial system. Twenty-nine (29) unconsolidated loose and friable sandstone samples were selected for textural analysis. Grain-size parameters such as mean, median, standard deviation, Skewness and Kurtosis were used for transport history, mode and hydrodynamic energy condition to recognize the depositional environment. Stewart Diagram shows deltaic/wave water process takes active role under the influence of wave process. Linear discriminant functions analysis show that the fluvial environment of deposition dominates and influences shallows water and beach environment. Passega diagram reveals that transport mode was rolling and suspension by the tractive current that shows the fluvio-deltaic to deltaic wave with the influence of wave depositional environment of Miocene-Pliocene (Neogene) Manchhar Formation.

KEYWORDS: Comparative Depositional Heterogeniety; Lithofacies; Grain Size Analysis; Manchhar Formation; Southern Indus Basin; Pakistan

*Corresponding author: (Email: aijaz.halepoto@usindh.edu.pk, Phone: 0092-3342048110)

1. INTRODUCTION

Depositional sedimentary environments provide vital constraints regarding paleo-geography, biodiversity and tectonic evolution. Different field and laboratory based approaches are being used to decipher the depositional environment of sedimentary rocks such as lithofacies, petrography, grain size analysis, mineralogy and geochemistry. Lithofacies and Grain size analysis are the essential techniques in sedimentology for extracting geological information from clastic sedimentary rocks to understand the paleo-climatic and environmental setting, hydrodynamics, transportation, and provenance of sediments [1-3]. Grain size parameters are broadly employed to interpret sediment's source, transportation mechanism and depositional environment and paleo-hydrodynamic setting [1, 4-9]. Some recent studies regarding interpretation of depositional environment by employing grain size analysis includes [10-15]. Various methods are used to measure the grain size of clastic sediments based on research and the extent of particle sizes to be measured. Direct grain size analysis and point counting are the two extensively used approaches for

particle size measurement [2, 4, 16]. The Sedimentologists concentrate on (a) type of grain size measuring method, (b) technique of computing textural data, and (c) representing in mathematical and graphical methods. The graphical technique involves producing textural data on bivariate graphs, and the mathematical treatment/method uses arithmetic equation or grain size parameters to correspond to textural data. In environmental studies, two-factor difference graphs and "Linear Discriminate Function" (henceforth LDF) and log probability graphs are widely used as graphical plots in textural studies. Drawing of two-factor deviation graph helps to differentiate between the various depositional environment [9, 17-19].

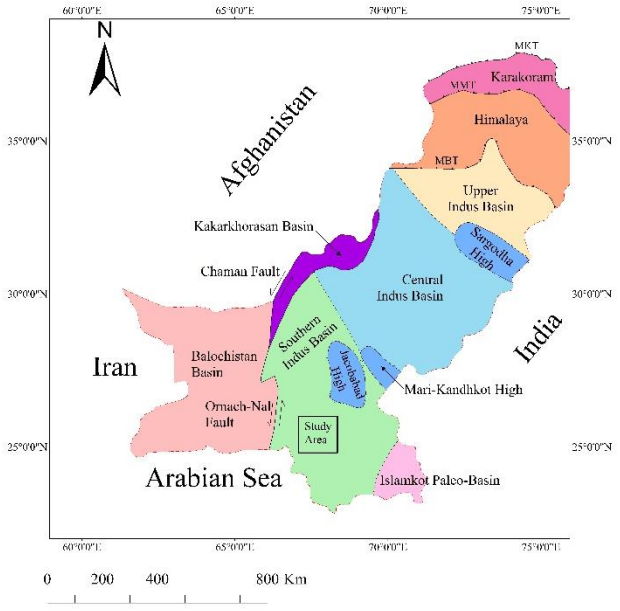

Figure 1. Map of Sedimentary Basins of Pakistan, showing study area, modified after [20-22].

The sediments of Manchhar Formation (Siwalik Group) of Miocene-Pliocene (henceforth Neogene) age have been focused for its geological setting to understand deformation of the Himalaya during that age. Still lot of work is needed to respond the inquiry regarding the depositional setting, paleo-climatic conditions, paleo-geographic setup and Himalayan orogeny; specifically in Southern Indus Basin. Therefore, an attempt has been made to resolve the various perspective regarding the depositional environment of sandstone of the Manchhar Formation from different sections (Fig.1) in Southern Indus Basin, using Lithofacies analysis and grain size analysis. The Neogene Molasses including Manchhar Formation are well exposed along the foot-hills of the Kirthar-Suleiman and Himalayan orogenic belt of Indian sub-continent. The Kirthar-Suleiman orogenic belts are located along the western margin of Indus Basin, while Himalayan orogenic belt is located along the northern margin of Indus Basin [21, 23].

Table 1. Stratigraphy of the Southern Indus Basin, after [22, 23].

Period		Group	Formation	Lithology
Quaternary	Holocene		Alluvium/Terrace	Mixed Clastics
	Pleistocene		Lei / Dada Conglomerate	Conglomerate
Tertiary	Mio-Pliocene	Siwalik Group	Manchar Formation	Sandstone, claystone, shale and conglomerate
	Miocene	Moman i Group	Gaj Formation	Sandstone, shale and limestone
	Oligocene		Nari Formation	Sandstone, shale and limestone
	Eocene		Kirthar Formation	Limestone
			Laki Formation	Limestone, minor shale and sandstone
	Paleocene	Ranikot Group	Lakhra Formation	Limestone with shale and sandstone
			Bara Formation	Sandstone with shale and volcanic debris
			Khadro Formation	Sandstone, shale, limestone
			Khaskheli Basalt	Basalt
Cretaceous		Mona Jhal Group	Moro Formation	Limestone, marl and shale
			Pab Sandstone	Sandstone with some marl and limestone
			Fort Munro Formation	Limestone and calcareous shale
			Mughalkot Formation	Calcareous mudstone and shale with limestone and sandstone
			Parh Limestone	Limestone with marl and shale
			Goru Formation	Limestone, shale, siltstone and sandstone
			Sembar Formation	Shale, siltstone and limestone
Jurassic			Takatu Formation	Limestone
			Anjira Formation	Limestone
			Shrinab Formation	Limestone
Triassic			Wulgai Formation	Shale, marl, claystone
Cambrian to Permian rocks are neither exposed nor drilled				
Precambrian		Nagarparkar Igneous Complex		Granite, rhyolite, gniess

The rifting of the Indian Plate from other Gondwanian fragments during the Mesozoic

created various realms of Tethys Ocean along the western margin of the Indian Plate and geology of Indus Basin mainly based on the rocks deposited in these realms of Tethys Ocean along the western margins [24, 25]. The Indus basin is divided into the Upper and Lower Indus Basin, separated by the Precambrian shield element Sargodha High [21] (Fig.1). Jacobabad High is another basement zone of unwrap that divides the Lower Indus Basin into Central and Southern Indus Basin [21, 23, 26] (Fig.1). The Precambrian crystalline basement rocks and sedimentary rocks of Mesozoic and Cenozoic are reported from the Southern Indus Basin [23, 24] (Table 1).

Manchhar Formation mainly comprises of inter-bedded sandstone, conglomerate, and subordinate shale. Sandstone is grey, greenish-grey, light greyish gritty, soft, crumbly fine to coarse and pebbly, flat and cross bedded. The sandstone proportion increases in the upper part of the formation. Shale is mild, earthy yellow, brownish and brick-red colored. Conglomerate consists of a pebble of sandstone and fossiliferous limestone. The Pebbles of conglomerates are sub-angular to sub-round. Manchhar Formation unconformable overlies the different Tertiary rocks and overlain by Pleistocene Dada Conglomerate of Holocene Terrace deposits. Neogene age is assigned to Manchhar Formation based on Mammal and wood fossils [27].

2. MATERIALS AND METHODS

Three stratigraphic sections of Manchhar Formation are measured through tape_brunton and Jacob's staff method [28, 29] (Fig. 2). Thirty-five unconsolidated sandstone and shale samples were collected through random sampling method (one bed-one sample) [28, 29]. Four lithofacies have been recognized based on the field parameters, i.e., texture, sedimentary structure, grain size, and lithologic units. For the detailed textural analysis these three sections were logged and properly sampled, mostly from unconsolidated sandstone beds, and twenty-nine (29) samples were selected for grain size analysis (Fig. 3). Uden and Wentworth millimeter scale of sediments converted into Φ-scale [30]. Cumulative frequency curves were produced from the cumulative weight percent of grain size data of each section. From these cumulative frequency curves, selected percentile values such as, 5, 16, 25, 50, 75, 84 and 95 were recorded and various grain size strictures, such as "mean, standard deviation, (sorting), skewness, and kurtosis" are computed. The software platforms of ArcGIS 10.3, Corel Draw X4, LogPlot 7 and Origin Pro 9 were used for maps, image annotations, lithofacies logs and grain size graphical plots respectively.

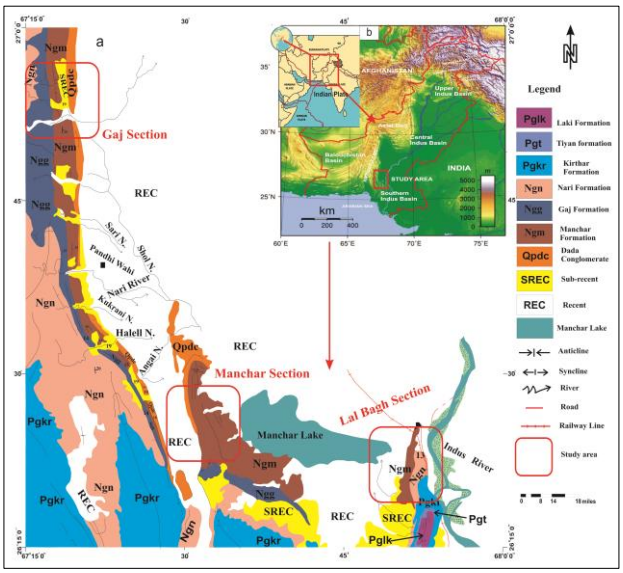

Figure 2. Geological map of the study area, modified after [27].

3. RESULTS AND DISCUSSION

The present study has successfully recognized four principle types of lithofacies (Gt, St, Sr, Fm) in the Manchhar Formation in the studied sections (Fig. 4). Studied sections show the principally clastic sedimentary rock lithology ranges from Conglomerate, Sandy Conglomerate, Sandstone and Shale. During present study the facies nomenclature is adopted as recommended by Miall [31].

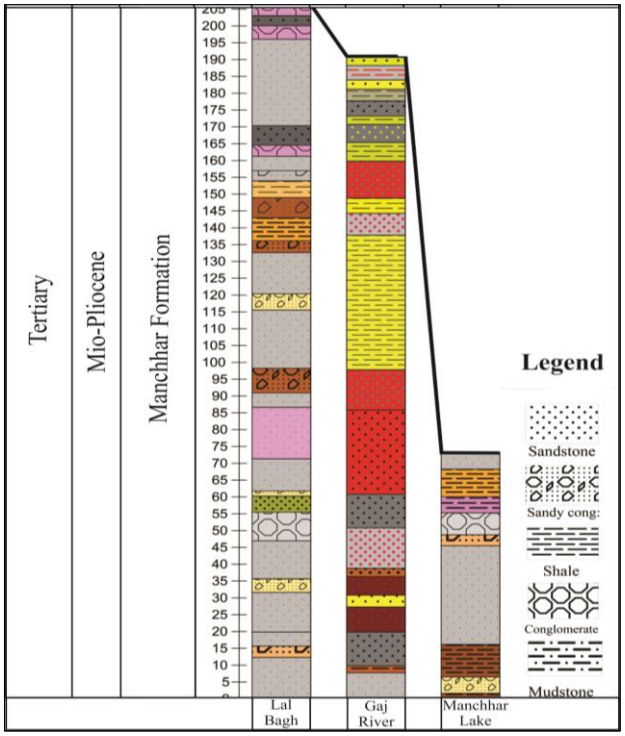

Figure 3. Measured Stratigraphic Sections Manchhar Formation Lower Indus Basin Pakistan.

3.1. Facies analysis

Depending on the grain size, sedimentary structures and vertical facies relationship, four facies were recognized in the Gaj, Manchhar and Lal Bagh sections of the Manchhar Formation. These lithofacies at studied sections showed variable thickness and were used to identify the depositional setting. Recorded lithofacies are described below.

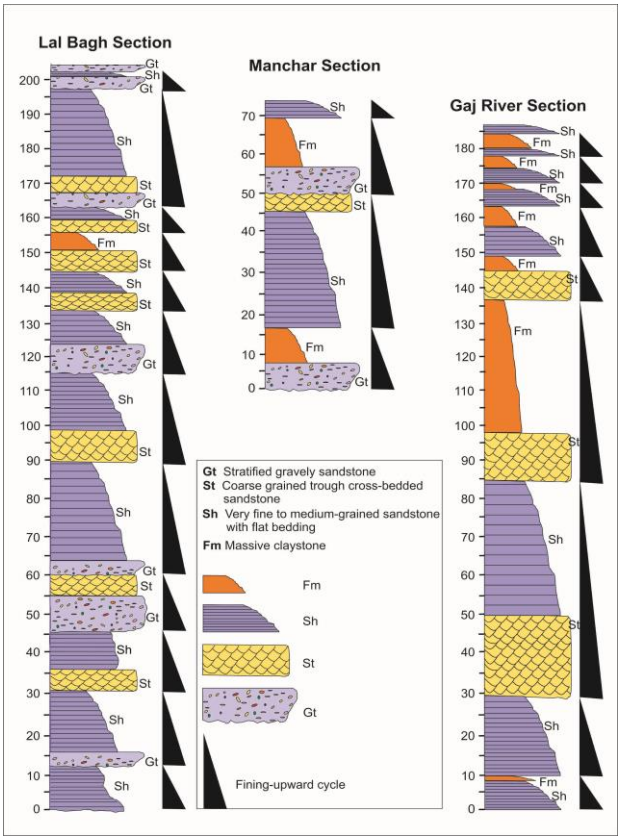

Figure 4. Stratigraphic sections of the Manchhar Formation showing the vertical relationship of facies.

3.1.1. Conglomeratic Sandstone (Gt)

Conglomeratic sandstone facies exist in the lower part of the Manchhar Formation that exhibit complete fining upward cycle. It is off white, grey, yellowish-grey, light brown, greyish-brown, yellowish-brown, light grey, and light brown. The grain size ranges from pebbles to medium sand, which are angular to sub-round, moderate to poorly sorted and friable (Fig. a, b & e). The facie is highly calcareous, and the matrix contains sand, silt and clay. Some channel conglomerate facies are fining upward to sandstone facies signifying either step by step retreating flow during diversion or regular lateral resettlement channel [31, 32]. This facies indicates that the conglomerate sandstone facies deposited in minor channel fill stream flow deposits. Still, it

also swiftly slow down the excess amount of gravel-dominated stream flow under flashy discharge [32-34].

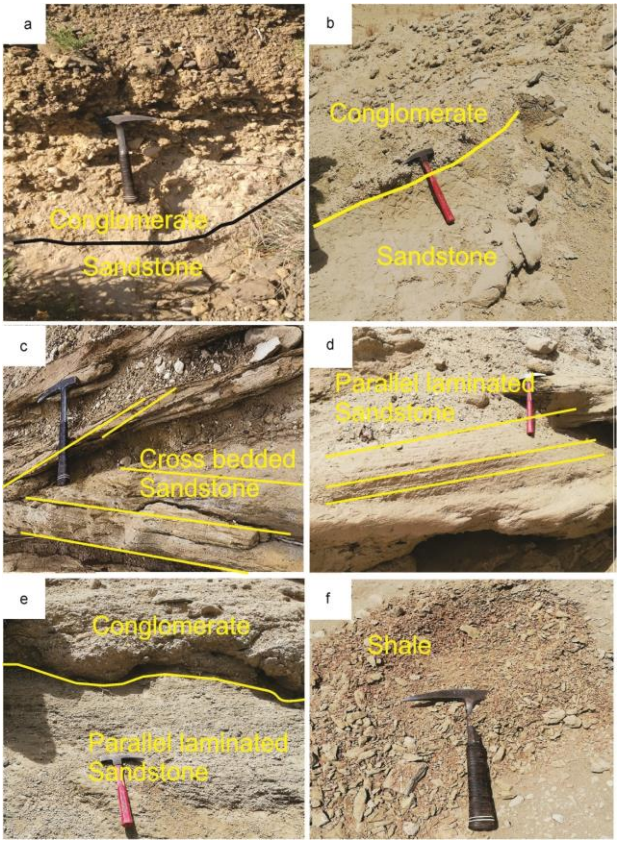

Figure 5. Field photographs showing (a) sandstone and conglomerate (b) sandstone and conglomerate (c) Trough cross bedded sandstone (d) planner cross-bedded sandstone (e) parallel-laminated sandstone and conglomerate (f) shale

Winnowing action in the thalweg of channel displaces the finer sediments and deposits the gravel [35-37]. Three processes are operating at channel base i.e. scouring/rubbing bedload transportation and deposition, whereas, creation of new floodplain channels results from repeated crevassing and avulsion [38, 39]. Laury [40] describes a cohesive overbank fall down mechanism involving shearing by rotational slumping, consequential in the brecciation of material below thalweg depth. The sandstone is thought to have been deposited on related floodplains as crevasse splay channels of a distant, sand-dominant braided fluvial system [32, 41, 42].

3.1.2. Shale (Fm)

Shale facies is composed of fine-grain of silt and clay-size mineral. The color ranges from bluish grey, grey, greyish, brownish grey to grey pinkish to camel color (Fig. 5f). It is soft, loose, oxidized and contains mud-cracks and plant rootlets. Iron oxide or iron hydroxide minerals such as hematite, goethite, or limonite are frequently found in shale deposited in oxygen-rich settings. Many varieties of shale have red, brown, or yellow colors due to a small percentage of these minerals dispersed throughout the rock. Red shale can be formed when hematite is present. Yellow or brown shale can result from the presence of limonite or goethite. The fine-grain components imply that a large amount of the sediment was accumulated in the flood plain area, based on the interpretation of lithological properties of this type of facies. Because of the abundance of burrows and calcareous concretion, the sandy silt and clay units are most likely levee-associated small terminal splay deposition [42-45]. The migration of calcareous solutions was facilitated by numerous burrows and rootless [46-48]. The sequence Manchhar Formation at Lal Bagh section is typical of a braided river system [49, 50]. Variability in the grain size reflects the difference in water stage fluctuations [31, 51].

3.1.3. Medium-fine grained sandstone (Sh)

These facies recognized in the Manchhar Formation at Lal Bagh section are flatbed thick to very thick-bedded sandstone. These facies are smoky white, yellowish, brownish, greenish grey, greenish-yellow, yellowish-brown, and

greyish. The grain size ranges from fine grain to medium-grained, which are rounded to sub-rounded and well-sorted to moderately well sorted and friable (Fig. 5d). They have no orderly variation of sedimentary structure, but burrows and rootlets tend to occur near the top. These lithofacies belong to weakly confined, and distributaries splay association/environment [34, 42, 52]. These facies are regarded as channel fill sediments and conceived as the depositing of crevasse splay channels in connected flood plains of a distant, sand-dominant braided fluvial system [32, 41, 53]. The crevasse splay channels were formed by repeated crevassing and incision, and the channel base encountered recurrent scouring, bed-load transportation, and sedimentation [38, 39]. The upward movement of shaly lenses, burrows, and root traces could be related to abandoning crevasse channels and diminishing current energy [31, 38, 50, 53-56].

3.1.4. Trough cross-bedded sandstone (St)

Fine to coarse grained trough cross-bedded sandstone facies are mostly repeated common in Manchhar Formation. It is generally greenish yellow, yellowish brown, greenish brown, dark brown, yellowish grey, greyish grey. It is thick-bedded and show fining upward pattern. Grains are angular to sub-round and moderate to poorly sorted (Fig. 5c). The facies is friable characterized by dominantly cross-bedded sandstone that is underlying conglomerate facies (Gt). This facies has clayey matrix having calcareous cement and become in places friable. Individual beds show limited fining-upward characteristics, which could be attributable to a lack of particle sizes heterogeneity.

The accumulation of a distal sand influential braided fluvial system is construed as fine-coarse grain trough cross-bedded sandstone facies. The lateral movement generated the large-scale inclined strata, which are channel bar deposits. The absence of mud cracks and roots evidence in the lowermost part of the channel deposits demonstrated perennial river flow [11, 57]. Trough and planer cross-stratification indicate the existence of a moving sinuous crested dune and a moving straight crested dune, respectively. The latter was discovered in the presence of higher flow velocities. The erosive power of many simultaneously active changing channels is likely to responsible for the failure of vertical accretion of sediments [41, 42, 51].

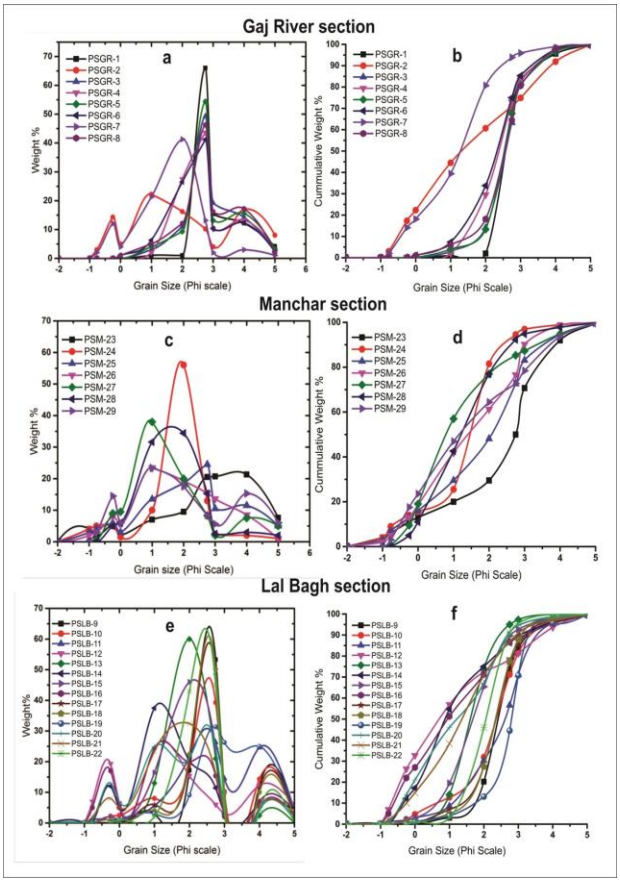

Figure 6. Grain-size distribution frequency curves (a, c & e) and cumulative frequency curves (b, d & f) for the Manchhar Formation.

Table 2. Summary of Grain Size Parameters. "Mz=Mean, SD=Standard Deviation (Sorting), SKI=Skewness, KG=Kurtosis, Svf=Very Fine Sand, Sf=Fine Sand, Sm=Medium Sand, PS=Poorly Sorted, MS=Moderately Sorted, MWS=Moderately Well Sorted, NS=Nearly Symmetrical, SFS=Strongly Fine Skewed, FS=Fine Skewed, CS=Coarse Skewed, SCS= Strongly Coarse Skewed, PK= Platykurtic, MK= Mesokurtic, LK= Leptokurtic, VLK= Very Leptokurtic".

S. No.	Sample Name	Mz	Verbal limits	SD	Verbal Limit	SKI	Verbal Limits	KG	Verbal Limits
1	PSGR-1	2.88	Sf	0.63	MWS	0.49	SFS	1.10	MK
2	PSGR-2	1.90	Sm	1.74	PS	0.13	FS	0.77	PK
3	PSGR-3	2.89	Sf	0.79	MS	0.17	FS	1.19	LK
4	PSGR-4	2.66	Sf	0.83	MS	0.26	FS	1.16	LK
5	PSGR-5	2.88	Sf	0.78	MS	0.26	FS	1.08	MK
6	PSGR-6	2.59	Sf	0.90	MS	0.15	FS	1.63	VLK
7	PSGR-7	1.4	Sm	1.12	PS	-0.27	CS	1.38	LK
8	PSGR-8	2.7	Sf	0.85	MS	0.12	FS	1.05	MK
9	PSLB-9	2.71	Sf	0.78	MS	0.26	FS	1.29	LK
10	PSLB-10	2.61	Sf	1.05	PS	0.07	NS	1.16	LK
11	PSLB-11	2.80	Sf	1.05	PS	0.04	NS	0.78	PK
12	PSLB-12	1.58	Sm	1.81	PS	0.20	FS	0.89	PK
13	PSLB-13	1.98	Sm	0.53	MWS	0.11	FS	1.21	LK
14	PSLB-14	1.59	Sm	1.27	PS	0.19	FS	1.59	VLK
15	PSLB-15	1.98	Sm	0.79	MS	0.28	FS	1.68	VLK
16	PSLB-16	1.34	Sm	1.49	PS	-0.005	NS	1.05	MK
17	PSLB-17	2.53	Sf	0.92	MS	0.08	NS	1.50	VLK
18	PSLB-18	2.61	Sf	0.72	MS	0.22	FS	1.38	LK
29	PSLB-19	3.09	Svf	0.84	MS	-0.004	NS	0.91	MK
20	PSLB-20	1.54	Sm	1.22	PS	-0.04	NS	1.12	LK
21	PSLB-21	1.79	Sm	1.17	PS	0.04	NS	1.43	LK
22	PSLB-22	1.96	Sm	0.79	MS	-0.09	NS	0.86	PK
23	PSM-23	2.64	Sf	1.16	PS	-0.32	SCS	1.20	LK
24	PSM-24	1.44	Sm	1.17	PS	0.44	SCS	2.85	VLK
25	PSM-25	2.06	Sf	1.63	PS	-0.18	CS	1.24	LK
26	PSM-26	1.93	Sm	1.59	PS	0.03	NS	1.04	MK
27	PSM-27	2.88	Sf	0.63	MWS	0.49	SFS	1.10	MK
28	PSM-28	2.49	Sf	0.90	MS	0.15	FS	0.63	VPK
29	PSM-29	1.78	Sm	1.73	PS	1.14	SFS	0.86	PK

3.2. Textural Analysis

3.2.1. Cumulative Frequency Curve

The cumulative frequency curve usually creates an S-shaped curve and the gradient of the cumulative frequency curves at the middle part reflects the sorting of sediments. Gentle or broad slop of curve indicates the poor sorting and reveals low hydrodynamic conditions, and steep slope indicates well sorting of sediments and indicates high hydrodynamic energy condition (Fig 6). Cumulative frequency curves indicates dominance unimodality around 2.5Φ for Gaj River Section (Fig. 6b), Manchhar Lake Section (Fig. 6d) and 2.0Φ for Lal Bagh Section (Fig. 6f). However, few samples indicate the bimodal with various frequency distribution around 0.5Φ. The dominance of the unimodal nature of sediments indicates the little bit of mixing of clay particles and suggests a relatively steady depositional mechanism. Some samples of studied sections indicates bimodality peaks at around 1.5Φ (Fig. 6a, c & e). The bimodal nature of sediments is characterized by a mixture of various grain sizes and depositional processes and the change in transportation mode. Grain size parameters of clastic sedimentary rocks, such as, mean size, median, standard deviation (Sorting), Kurtosis and Skewness play an essential role in understanding sediments depositional mechanism [4, 12, 58, 59].

3.2.2. Interpretation of Graphic Mean

Graphic mean size represents the average grain size of sediments. The studied section indicates that fine sand was dominant over medium sand in Manchhar Lake and Gaj River sections. In contrast, medium sand was prevalent over the fine sand in the Lal Bagh Section. In the studied sections, the graphic mean size ranges between 1.34 to 3.09Φ.

The inclusive graphic standard deviation or sorting is one of the most valuable processes to find out the nature of the sorting or uniformity in sediments and indicate hydrodynamic conditions during transportation and deposition [2, 13]. The results of the studied section (Table 2) reveal that poorly sorted sediments are dominant over moderately sorted sediments indicative of moderate to high hydrodynamic energy conditions [12, 59].

Kurtosis indicates sharpness or peakedness in the frequency distribution curve of grain size by measuring the ratios between the sorting in the "tails" of the curve and the sorting in the central portion. The results of Kurtosis for studied sections varied between 0.63 to 2.85Φ (Table 2). The sharpness or peakedness (Kurtosis) mainly was dominant with Lepokurtic behavior, followed by very leptokurtic, Platykurtic, Mesokurtic and very Platykurtic [1, 59].

Skewness depicts the consistency/uniformity in the supply of sediments in most fine or coarse proportions. Skewness results for study sections range from between -0.005 to 1.14 Φ (Table 2), indicating the dominance of fine skewed, followed by nearly symmetrical, strongly fine skewed, strongly coarse skewed and coarse skewed [6, 13, 58].

3.2.3. Interpretation of Bivariate diagrams

The bivariate plot of sorting versus mean (Mz) indicates that the samples of studied sections are fine to medium sand size and poorly to moderately well sorted [59, 60]. Which most of the sample of Manchhar Formation poorly sorted to moderately sorted and are fine sand to medium sand. The samples of the Gaj River Section are primarily fine sand and moderately sorted, possibly due to grain to grain interaction perhaps grains decrease and moderately

sorted. The samples of the Lal Bagh Section dominantly medium grain sand and poor to moderately sorted whereas, samples of the Manchhar Lake Section are primarily fine sand and poorly sorted (Fig. 7a). The dominance of poorly sorted to moderately sorted sandstones in the Manchhar Formation may point to a near-source region [11, 14, 61].

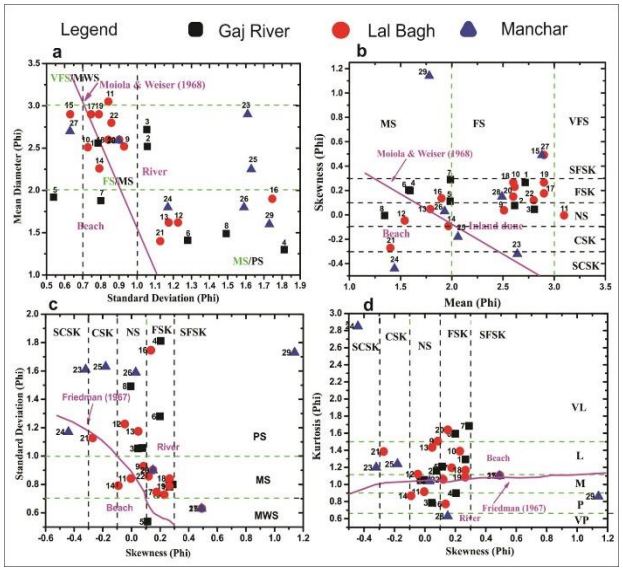

Figure 7. (a) Bivariate plot of Standard Deviation against Mean, (b) Mean against Skewness, (c) Skewness versus Standard Deviation and (d) Skewness versus Kurtosis.

The skewness value was plotted against graphic mean following [60] demonstrate that most of Manchhar Formation sediments are fine skewed to near symmetrical in nature and minority are fall in strongly fine skewed and coarse skewed. This diagram confirms most of the Manchhar Formation samples are fine sand to medium sand grain [13, 59]. Figure 7b indicates that most samples of studied sections clustered in inland dune field and some samples gathered in the beach environment.

The sorting plotted against graphic Skewness confirms that most Manchhar Formation samples are poorly sorted to moderately sorted and fine skewed to near-symmetrical are fall in coarse skewed [6, 59] (Fig. 7c).

The plot of graphic kurtosis versus skewness reveals that almost all samples are leptokurtic to mesokurtic followed very leptokurtic to platykurtic and mostly near symmetrical to fine skewed (Fig. 7d). The excess and lowest values of kurtosis reveal that some samples acquire their sorting at somewhere else in the depositional environment [4, 14, 17]. Interms of depositional environment scatter plot of graphic kurtosis versus skewness reveals that dominant influence of beach environment over riverine [59].

Various attempts have been made to set up a link between statistical parameters and depositional environment [8, 16, 17, 60, 62, 63]. Scatter graphs are produced on the assumption that statistical parameters reliably indicates variation in hydrodynamic conditions of transportation and sedimentation [44].

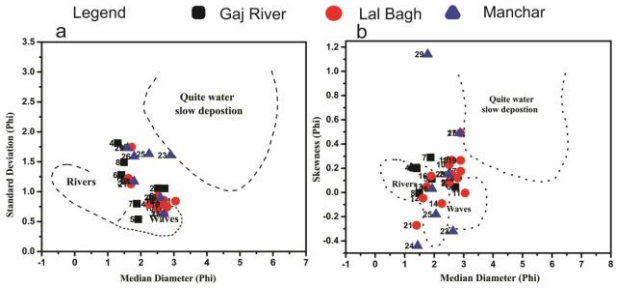

Figure 8. (a) Bivariate plot of graphic median versus standard deviation. (b) Bivariate plot of Skewness versus median.

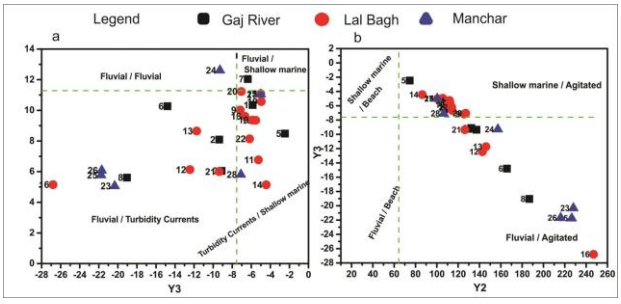

Figure 9. (a) Discrimination of environments based on Linear Discrimination functions plot of Y_4 against Y_3, (b) Discrimination of environments based on Linear Discrimination functions plot of Y_2 against Y_3.

Table 3. Calculated Linear Discriminate Functions of Manchhar Formation. "S.No. =Sample Number, B=Beach, D=Deltaic, SM=Shallow Marine, SAW= Shallow agitated water, TC= Turbidity Currents".

S. No.	Y_1	Y_2	Y_3	Y_4	Y_1	Y_2	Y_3	Y_4
1	-3.94	111.72	-5.86	10.35	SAW	SM	SM	D
2	-1.74	137.15	-9.36	8.09	B	SM	D	TC
3	-3.55	132.29	-9.12	6.05	SAW	SM	D	TC
4	8.89	260.79	-29.27	5.95	B	SM	D	TC
5	-2.47	74.56	-2.47	8.48	B	SM	SM	TC
6	4.93	165.69	-14.8	10.27	B	SM	D	D
7	-0.08	109.51	-6.37	12.04	B	SM	SM	D
8	6.73	186.66	-19.04	5.61	B	SM	D	TC
9	-1.35	125.69	-7.16	10.02	B	SM	SM	D
10	-3.52	105.59	-4.95	10.57	SAW	SM	SM	D
11	-5.57	111.9	-5.26	6.77	SAW	SM	SM	TC
12	3.65	142.73	-12.44	6.13	B	SM	D	TC
13	3.08	146.05	-11.73	8.65	B	SM	D	TC
14	-1.81	86.35	-4.44	5.14	B	SM	SM	TC
15	-6.41	100.66	-5.01	11.09	SAW	SM	SM	D
16	6.61	246.96	-26.8	5.15	B	SM	D	TC
17	-4.63	112.36	-5.54	9.35	SAW	SM	SM	TC
18	-3.82	114.42	-6.66	9.61	SAW	SM	SM	TC
19	-5.14	110.88	-5.88	9.36	SAW	SM	SM	TC
20	-1.44	127.1	-7.05	11.23	B	SM	SM	D
21	4.59	126.25	-9.36	6	B	SM	D	TC
22	-4.22	113.94	-6.18	8.14	SAW	SM	SM	TC
23	4.57	228.06	-20.33	5.06	B	SM	D	TC
24	9.72	157.26	-9.29	12.61	B	SM	D	D
25	6.72	226.51	-21.75	5.77	B	SM	D	TC
26	5.65	216.12	-21.69	6.08	B	SM	D	TC
27	-6.4	100.39	-5	11.04	SAW	SM	SM	D
28	-4.24	106.58	-7.09	5.81	SAW	SM	SM	TC
29	5.04	261.08	-31.25	12.3	B	SM	D	D

The discriminate diagram (Fig. 8) was proposed by Stewart [62] to understand the energy condition and deposition of sediments and differentiate among the river, wave, and slow water processes by producing a graph between the skewness versus median. It has been recognized that almost all Manchhar Formation sandstone samples fall between the river field and relatively slow water deposition and some samples fall in the wave field and river field (Fig. 8a). All the Manchhar Formation sandstone samples scattered in and around the wave field and river field, which reveals that they were deposited by the deltaic/wave process [6, 59] (Fig. 8b).

Textural parameters of statistical analysis was applied to be used to identify hydrodynamic conditions throughout the sedimentary processes. It seems to have a perfect relationship to different depositional settings [8]. Sahu [8] produced and formulated the function known as LDF Y_1, Y_2, Y_3 and Y_4. LDF functions were used to discriminate among deposition mechanisms. LDF were computed from the calculated textural parameters (Table 3).

The scatter graph Y_3 versus Y_2 proposed by Sahu [8] (Fig. 9b) reveals that most sediments of the Manchhar Formation plummet in the field of "shallow marine/agitated environment". Some samples are huddled in the field of the "fluvial/agitated" depositional setting domain. The bivariate plot of Y_4 versus Y_3 (Fig. 9a) shows that most sediments gathered in the field of "shallow marine/turbidity current" depositional setting. Moreover, some samples occupy "turbidity currents/fluvial environment". This indicates that the sediments are deposited in a "fluvial to deltaic depositional environment" with the influence of "shallow marine environments" [1, 59].

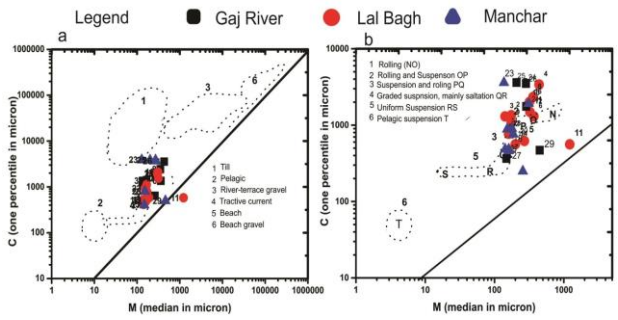

Figure 10a&b. C-M plots showing the transporting mechanism of the Manchhar Formation.

C-M diagram is used to understand the hydrodynamical conditions that prevail during sedimentation proposed by Passega [63]. The plot is a two-fold graph in which "C" denotes one-percentile in microns and "M" denotes median in microns on a logarithm scale. Passega recommended that the ratio of C to M is an indicator of depositional environment hydrodynamics. C-M graph suggests that the sandstone of the Manchhar Formation is deposited under tractive currents near the beach environment (Fig. 10a). C-M graph (Fig. 10b) reveals that most of the samples from the Manchhar Formation clustered in rolling and suspension field (PQ), some samples gathered rolling field (NO) and few samples fall in the suspension and rolling field (QP) [1, 59].

4. CONCLUSION

The Manchhar Formation (Neogene Molasses of Siwalik Group) in study area is mainly composed of clastic sediments. Facies evidences and grain size distribution diagrams suggest that Manchhar Formation have been deposited in shallow agitated water of beach to delta and fluvial system. Furthermore, diagrams also suggest that sediments of Manchhar Formation were mainly transported through rolling and suspension.

DECLARATIONS

Funding: No funding is availed for this study.

Conflicts of interest / Competing interests: The authors declare no any conflict of interest or competing interests to disclose.

Data availability: Not applicable

Code availability: Not applicable

Authors' contributions:

Asghar A. A. D. Hakro, Abdul Shakoor Mastoi & Rafique Ahmed Lashari: Conceptualization, Supervision and Methodology. **Muhammad Soomar Samtio, Aijaz Ali Halepoto, & Mushtaque Ahmed Rahoo**: Data Collection, Processing, Draft Preparation. **Riaz Hussain Rajpar:** Visualization, Software, Validation and Reviewing.

REFERENCES

[1] C. Baiyegunhi, K. Liu, O. Gwavava, Grain size statistics and depositional pattern of the Ecca Group sandstones, Karoo Super group in the Eastern Cape Province, Open Geosciences, (2017).

[2] M.S. Samtio, A.A.A.D. Hakro, R.A. Lashari, A.S. Mastoi, R.H. Rajper, M.H. Agheem, Depositional environment of Nari formation from Lal Bagh section of Sehwan area, Sindh Pakistan, Sindh University Research Journal,(Science Series), 53 (2021) 67-75.

[3] M.A. Quasim, S.K. Ghosh, A.H.M. Ahmad, V.K. Srivastava, M. Albaroot, Integrated approach of lithofacies and granulometric analysis of the sediments of the Proterozoic Upper Kaimur Group of Vindhyan Supergroup, Son Valley, India: Palaeo-environmental implications, Geological Journal, 55 (2020) 5991-6012.

[4] T.L. Baiyegunhi, K. Liu, O. Gwavava, C. Baiyegunhi, Textural characteristics, mode of transportation and depositional environment of the Cretaceous sandstone in the Bredasdorp Basin, off the south coast of South Africa: Evidence from grain size analysis, Open Geosciences, 12 (2020) 1512-1532.

[5] S. Boggs, Petrology of Sedimentary Rocks, Cambridge University Press, 2009.

[6] M.S. Samtio, Hakro, A. A. A. D., Mastoi, A. S., Rajper, R. H., and Nangraj, A, Depositional Pattern of the Siwalik Group (Manchar Formation) Southwest of LalBagh, Sehwan Area, Sindh, Pakistan, Sindh University Research Journal -Science Series,, 52 (2020) 363–368.

[7] A.A. Ghaznavi, M. Quasim, A. Ahmad, S.K. Ghosh, Granulometric and facies analysis of Middle–Upper Jurassic rocks of Ler Dome, Kachchh, western India: an attempt to reconstruct the depositional environment, Geologos, 25 (2019) 51-73.

[8] B.K. Sahu, Depositional mechanisms from the size analysis of clastic sediments, Journal of Sedimentary Research, 34 (1964) 73-83.

[9] G.S. Visher, Grain size distributions and depositional processes, Journal of Sedimentary Research, 39 (1969).

[10] A. Duquesne, J.-M. Carozza, Improving Grain Size Analysis to Characterize Sedimentary Processes in a Low-Energy River: A Case Study of the Charente River (Southwest France), Applied Sciences, 13 (2023) 8061.

[11] A. Dawelbeit, E. Jaillard, A. Eisawi, Grain size analysis of the latest Quaternary Kordofan Sand of Central Sudan: Depositional environment and mode of transportation, Aeolian Research, 55 (2022) 100785.

[12] R. Khalil, Grain-Size Analysis of Middle Cretaceous Sandstone Reservoirs, the Wasia Formation, Riyadh Province, Saudi Arabia, Sustainability, 15 (2023) 7983.

[13] U. Perera, A.S. Ratnayake, W. Weerasingha, H. Subasinghe, T. Wijewardhana, Grain size distribution of modern beach sediments in Sri Lanka, Anthropocene Coasts, 6 (2023) 10.

[14] S. Ghadeer, Grain size analysis and characterization of sedimentary environment of the surface sediments along the Syrian Coast, Umm al-Tuyour (Latakia), Marine Georesources & Geotechnology, (2022) 1-8.

[15] T. Chitkara, O. Thakur, A. Sharma, Textural Characteristics and Depositional Environment of a Late Quaternary Alluvial Plain of Haryana, Open Journal of Geology, 12 (2022) 870-882.

[16] G.M. Friedman, Dynamic processes and statistical parameters compared for size frequency distribution of beach and river sands, Journal of Sedimentary Research, 37 (1967) 327-354.

[17] G.M. Friedman, Distinction between dune, beach, and river sands from their textural characteristics, Journal of Sedimentary Research, 31 (1961) 514-529.

[18] K.-M. Sagoe, G.S. Visher, Population breaks in grain-size distributions of sand; a theoretical model, Journal of Sedimentary Research, 47 (1977) 285-310.

[19] G.M. Friedman, Differences in size distributions of populations of particles among sands of various origins: addendum to IAS Presidential Address, Sedimentology, 26 (1979) 859-862.

[20] M. Humayon, Lillie, R. J. and Lawrence, R. D., Structural Interpretation of the Eastern Suleiman Foldbelt and Foredeep, Pakistan, Tectonics, 10 (1991) 299–324.

[21] I.B. Kadri, Petroleum geology of Pakistan, Pakistan Petroleum Limited, 1995.

[22] N.K. Siddiqui, Petroleum Geology, Basin Architecture and Stratigraphy of Pakistan, Published by the Author, 2016.

[23] S.I. Shah, Stratigraphy of Pakistan (Memoirs of the Geological Survey of Pakistan), Geological Survey Of Pakistan, 2009.

[24] A.A. Hakro, W. Xiao, Z. Yan, A.S. Mastoi, Provenance and tectonic setting of Early Eocene Sohnari Member of Laki Formation from southern Indus Basin of Pakistan, Geological Journal, (2017).

[25] A.A.A.D. Hakro, M.S. Samtio, A.S. Mastoi, R.H. Rajper, The major elemental composition of middle paleocene sediments of southern Indus basin Pakistan: Implication on provenance, Earth Science Malaysia (ESMY), 5 (2021) 10-18.

[26] M.Q. Jan, A. Laghari, M.A. Khan, M.H. Agheem, T. Khan, Petrology of calc-alkaline/adakitic basement hosting A-type Neoproterozoic granites of the Malani igneous suite in Nagar Parkar, SE Sindh, Pakistan, Arabian Journal of Geosciences, 11 (2018) 1-14.

[27] H.S. Corporation, Reconnaissance Geology of Part of West Pakistan, A Colombo Plan Co-operative Project, Toronto, Canada., 1960.

[28] A.L. Coe, Geological field techniques, John Wiley & Sons, 2010.

[29] R.R. Compton, Manual of field geology, 1962.

[30] W.C. Krumbein, Size frequency distributions of sediments, Journal of sedimentary Research, 4 (1934) 65-77.

[31] A.D. Miall, Architectural-element analysis: a new method of facies analysis applied to fluvial deposits, Earth-Science Reviews, 22 (1985) 261-308.

[32] R. Sasmal, S. Bhattacharya, Lithofacies and Depositional Environments of the Garubathan Alluvial Fan, North Bengal, India, Journal of the Geological Society of India, 99 (2023) 495-508.

[33] R. Walker, Facies models: Geoscience Canada Reprint Series 1, Geol. Soc. Canada, Waterloo, 142p, (1979).

[34] M.E. Tucker, S.J. Jones, Sedimentary petrology, John Wiley & Sons, 2023.

[35] J.R. Allen, A review of the origin and characteristics of recent alluvial sediments, Sedimentology, 5 (1965) 89-191.

[36] J.R. Beerbower, Cyclothems and cyclic depositional mechanisms in alluvial plain sedimentation, Kansas Geological Survey Bulletin, 169 (1964) 31-32.

[37] S. Boggs, Principles of sedimentology and stratigraphy, (2012).

[38] N.D. Smith, Flume experiments on the durability of mud clasts, Journal of Sedimentary Research, 42 (1972).

[39] B. Makaske, D.G. Smith, H.J. Berendsen, Avulsions, channel evolution and floodplain sedimentation rates of the anastomosing upper Columbia River, British Columbia, Canada, Sedimentology, 49 (2002) 1049-1071.

[40] R.L. Laury, Stream bank failure and rotational slumping: preservation and significance in the geologic record, Geological Society of America Bulletin, 82 (1971) 1251-1266.

[41] P.G. DeCelles, K.A. Giles, Foreland basin systems, Basin research, 8 (1996) 105-123.

[42] M. Blum, S. Marriott, S. Leclair, Fluvial sedimentology VII, John Wiley & Sons, 2009.

[43] J.M. Coleman, Brahmaputra River: channel processes and sedimentation, Sedimentary geology, 3 (1969) 129-239.

[44] R.A. Sutherland, C.T. LEE, Discrimination between coastal subenvironments using textural characteristics, Sedimentology, 41 (1994) 1133-1145.

[45] Z. Chen, X. Li, H. Chen, Z. Duan, Z. Qiu, X. Zhou, Y. Hou, The Characteristics of Lithofacies and Depositional Model of Fine-Grained Sedimentary Rocks in the Ordos Basin, China, Energies, 16 (2023) 2390.

[46] M. Etheridge, J. Wilkie, An assessment of dynamically recrystallized grainsize as a palaeopiezometer in quartz-bearing mylonite zones, Tectonophysics, 78 (1981) 475-508.

[47] D.R. Prothero, F. Schwab, Sedimentary geology, Macmillan, 2004.

[48] G. Nichols, Sedimentology and stratigraphy, John Wiley & Sons, 2009.

[49] A.D. Miall, A review of the braided-river depositional environment, Earth-Science Reviews, 13 (1977) 1-62.

[50] S.K. Ghosh, Cyclicity and facies characteristics of alluvial sediments in the Upper Paleozoic Monongahela-Dunkard Groups, central West Virginia, in: F.G.E.R.M.F.M.D. Harvey (Ed.) Recent Developments in Fluvial Sedimentology, SEPM Society for Sedimentary Geology, 1987.

[51] I. Cojan, Alternating fluvial and lacustrine sedimentation: tectonic and climatic controls (Provence Basin, S. France, Upper Cretaceous/Palaeocene), Alluvial sedimentation, (1993) 425-438.

[52] A. Sprague, T. Garfield, F. Goulding, R. Beaubouef, M. Sullivan, C. Rossen, K. Campion, D. Sickafoose, V. Abreu, M. Schellpeper, Integrated slope channel depositional models: the key to successful prediction of reservoir presence and quality in offshore West Africa, Veracruz, Mexico, Colegio de Ingenenieros Petroleros de México, (2005) 1-13.

[53] J.J. Smith, B.F. Platt, Reconstructing late Miocene depositional environments in the central High Plains, USA: Lithofacies and architectural elements of the Ogallala Formation, Sedimentary Geology, 443 (2023) 106303.

[54] J. Bridge, S. Mackey, A revised alluvial stratigraphy model, Alluvial Sedimentation, (1993) 317-336.

[55] M.A. Pathan, M. Maira, J. MUET, Geology & Engineering Properties of Nagar Parkar Granites, District Tharparkar, Sindh, Pakistan, International Journal of Engineering Science, 18640 (2018).

[56] M. Mehmood, A.A. Naseem, M. Saleem, J.u. Rehman, G. Kontakiotis, H.T. Janjuhah,

E.U. Khan, A. Antonarakou, I. Khan, A.u. Rehman, Sedimentary Facies, Architectural Elements, and Depositional Environments of the Maastrichtian Pab Formation in the Rakhi Gorge, Eastern Sulaiman Ranges, Pakistan, Journal of Marine Science and Engineering, 11 (2023) 726.

[57] J. Quade, T.E. Cerling, Expansion of C4 grasses in the late Miocene of northern Pakistan: evidence from stable isotopes in paleosols, Palaeogeography, Palaeoclimatology, Palaeoecology, 115 (1995) 91-116.

[58] R.L. Folk, Petrology of sedimentary rocks, Hemphill publishing company, 1980.

[59] A.A.A.D. Hakro, W. Xiao, A.S. Mastoi, Z. Yan, M.S. Samtio, R.H. Rajper, Grain size analysis of the Oligocene Nari Formation sandstone in the Laki Range, southern Indus Basin, Pakistan: Implications for depositional setting, Geological Journal, (2021) 1-12.

[60] R.L. Folk, W.C. Ward, Brazos River bar: a study in the significance of grain size parameters, Journal of Sedimentary Research, 27 (1957) 3-26.

[61] R. Moiola, D. Weiser, Textural parameters; an evaluation, Journal of Sedimentary Research, 38 (1968) 45-53.

[62] H.B. Stewart Jr, Sedimentary reflections of depositional environment in San Miguel lagoon, Baja California, Mexico, AAPG bulletin, 42 (1958) 2567-2618.

[63] R. Passega, Grain size representation by CM patterns as a geologic tool, Journal of Sedimentary Research, 34 (1964) 830-847.

Received: 31 March 2023. Revised/Accepted: 11 December 2023.